Title

Bioorthogonal, Fluorogenic Targeting of Voltage-Sensitive Fluorophores for Visualizing Membrane Potential Dynamics in Cellular Organelles

Journal

Journal of the American Chemical Society, 144(27)

ISSN

0002-7863

Authors

Klier, Pavel EZ
Gest, Anneliese MM
Martin, Julia G
et al.

Publication Date

2022-07-13

DOI

10.1021/jacs.2c02664

Peer reviewed

HHS Public Access

Author manuscript

J Am Chem Soc. Author manuscript; available in PMC 2023 July 13.

Published in final edited form as:

J Am Chem Soc. 2022 July 13; 144(27): 12138–12146. doi:10.1021/jacs.2c02664.

Bioorthogonal, fluorogenic targeting of voltage-sensitive fluorophores for visualizing membrane potential dynamics in cellular organelles

Pavel E. Z. Klier[‡], **Anneliese M. M. Gest**[‡], **Julia G. Martin**[‡], **Ryan Roo**[‡], **Marisol X. Navarro**[‡], **Lauren Lesiak**[‡], **Parker E. Deal**[‡], **Neville Dadina**[‡], **Jonathan Tyson**[‡], **Alanna Schepartz**[‡,§], **Evan W. Miller**[‡,§,†,*]

[‡]Department of Chemistry, University of California, Berkeley, California, 94720, United States of America

[§]Department of Molecular & Cell Biology, University of California, Berkeley, California, 94720, United States of America

[†]Helen Wills Neuroscience Institute, University of California, Berkeley, California 94720, United States of America.

Abstract

Electrical potential differences across lipid bilayers play foundational roles in cellular physiology. Plasma membrane voltage is the most widely studied; however, the bilayers of organelles like mitochondria, lysosomes, nuclei, and endoplasmic reticulum (ER) also provide opportunities for ionic compartmentalization and the generation of transmembrane potentials. Unlike plasma membranes, organellar bilayers, cloistered within the cell, remain recalcitrant to traditional approaches like patch-clamp electrophysiology. To address the challenge of monitoring changes in organelle membrane potential, we describe the design, synthesis, and application of LUnAR RhoVR (**L**igation **Un**quenched for **A**ctivation and **R**edistribution **Rho**damine based **V**oltage **R**eporter) for optically monitoring membrane potential changes in the endoplasmic reticulum (ER) of living cells. We pair a tetrazine-quenched RhoVR for voltage sensing with a transcyclooctene (TCO)-conjugated ceramide (Cer-TCO) for targeting to the ER. Bright fluorescence is observed only at the coincidence of LUnAR RhoVR and TCO in the ER, minimizing non-specific, off-target fluorescence. We show that the product of LUnAR RhoVR and Cer-TCO is voltage sensitive and that LUnAR RhoVR can be targeted to intact ER in living cells. Using LUnAR RhoVR, we use two-color, ER-localized, fast voltage imaging coupled with cytosolic Ca^{2+} imaging to validate the electroneutrality of Ca^{2+} release from internal stores. Finally, we use LUnAR RhoVR to directly visualize functional coupling between plasma-ER membrane in patch clamped cell lines, providing the first direct evidence of the sign of the ER potential response to plasma membrane potential changes. We envision that LUnAR RhoVR, along with other existing organelle-targeting TCO probes, could be applied widely for exploring organelle physiology.

[*]***Corresponding Author***: evanwmiller@berkeley.edu.

Supporting Information. Experimental details, supporting figures, and spectra. This material is available free of charge via the Internet at http://pubs.acs.org.

Graphical Abstract

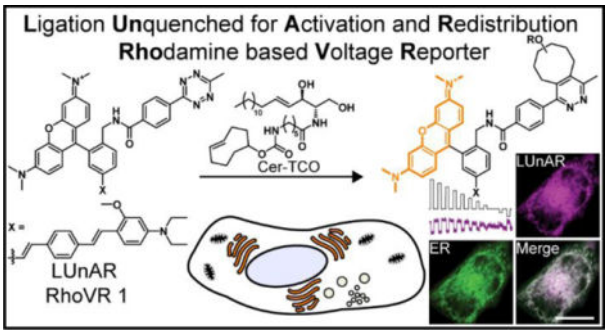

Introduction

Electrical potentials across biological membranes, including those that form membrane-bound organelles, regulate and initiate a host of physiological processes.[1] Although electrical potentials across external plasma membranes have been extensively studied, organelle membrane potentials remain relatively under-explored, by comparison. The membranes of organelles, ensconced within the confines of the cellular membrane, are difficult to access with electrodes, making determination of organelle membrane potential difficult.[2–4] While optical methods for monitoring changes in or measuring values of *plasma* membrane potentials are a powerful complement to electrode-based methods, delivering and targeting voltage-sensitive dyes to specific, internal organelle membranes for visualizing organelle membrane potential is an outstanding challenge.

Many strategies exist to target voltage sensitive fluorophores to mitochondria: most rely on lipophilic, cationic groups which accumulate in the mitochondrial matrix in a potential-dependent fashion. Approaches to other organelles are limited and most often involve bulk measurements of isolated organelle extracts.[5–7] Recent efforts to optically image membrane potential of internal organelles in intact cells have used DNA nanodevices[8] or genetic targeting with small molecule quenchers to target lysosomal membranes.[9] Other approaches use completely genetically encoded voltage-sensitive fluorescent proteins which express in both external and internal membranes to track membrane potential, but labeling can be ambiguous because of variable expression levels.[10] A need exists for robust approaches to monitoring membrane potentials of cellular organelles.

We wondered whether we might adapt VoltageFluor dyes for delivery to organelle membranes and take advantage of the photoinduced electron transfer (PeT) voltage-sensing mechanism to monitor membrane potential in organelles. Most existing VoltageFluors are designed to be cell impermeant for measuring cellular membrane potential and thus do not effectively stain organelle membranes.[11] However, we recently found that modifications to a rhodamine-based voltage reporter (RhoVR) enabled passage through cell membranes and localization to mitochondria.[12]

Fluorescent dyes can be targeted to subcellular locations either through charge,[13–15] covalently attached groups specific to a subcellular location,[16] genetic targeting of protein

constructs,[17–21] or bioorthogonal chemistry in which one reaction partner is attached to a targeting group and another is attached to the fluorescent probe to allow targeting in living cells.[22] A VoltageFluor targeted using bioorthogonal chemistry would be targetable to multiple subcellular locations using different targeted reaction partners. We selected a transcyclooctene (TCO)/tetrazine click reaction to use for subcellular targeting of VoltageFluors due to its rapid reaction kinetics[23–25] and the ability of tetrazines to quench the fluorescence of xanthene dyes.[26–28] Fluorescence becomes unquenched after the tetrazine group reacts with a strained alkene to form a covalent adduct, tethering unquenched dye to the subcellular location targeted by the alkene. We hypothesized that this could be general strategy for targeting and measuring membrane potential dynamics in internal organelles. A recent report described coupling of plasma membrane and internal membrane potential changes, and we thought a chemical targeting strategy along with a fast-response indicator like RhoVR might provide insight into this phenomenon.[10]

Results and Discussion

To realize this strategy, we made a **L**igation **Un**quenched for **A**ctivation and **R**edistribution **Rho**damine **V**oltage **R**eporter (LUnAR RhoVR). In this approach, a TCO is targeted to the membrane of interest using either a chemical targeting group or genetically targeted protein, after which the voltage reporter reacts with the targeted TCO to covalently bind it to the membrane of interest. Off-target background fluorescence is minimized because of quenching by the unreacted tetrazine group, (Scheme 1). After synthesizing and screening four different rhodamine-tetrazine linker chemistries for fluorescence turn-on (Figure S1), we settled on an amide linkage between the RhoVR and the tetrazine due to its superior turn-on and synthetic compatibility with published VoltageFluor syntheses (Scheme 1). Although direct conjugation of tetrazines to the pendant ring of the xanthene dyes give large fluorgenic responses (~100× fold)[27] via a through bond energy transfer mechanism (TBET),[29] amide-linked tetrazines afforded synthetic tractability and resonable unquenching responses ranging from 3× to 20× increase in fluorescence.[20, 30]

The synthesis of tetrazine-containing LUnAR RhoVR proceeds from a reduction of a brominated carboxytetramethyl rhodamine (**1**)[11] to the corresponding alcohol (**2**) followed by a Heck reaction with a molecular wire. The alcohol is then converted to a primary amine and coupled using car-bodiimide chemistry to 3-methyl-6-carboxyphenyl tetrazine(**24**)[31] to give LUnAR RhoVR 1 (Scheme 2). A similar synthesis with a molecular wire lacking aniline and methoxy groups gives LUnAR RhoVR 0, a voltage insensitive compound which serves as a useful control for cellular studies.[32–34]

LUnAR RhoVR 1 and 0 possess absorbance and emission spectra characteristic of tetramethyl rhodamine, with absorbance centered at 557 nm and an emission maximum of 578 nm (Figure 1, Figure S2). The fluorescence of LUnAR RhoVR 1 increases 7-fold upon reaction with TCO-ol (**25**); LUnAR RhoVR 0 increases 10-fold (Figure 1, Table 1). Although the fluorescence increases, the absorbance shows very little change before and after reaction with TCO (Figure 1), indicating that the increase in brightness results primarily from a change in the quantum yield of fluorescence. Similar turn-on ratios are achieved with TCO compounds bearing HaloTag ligands and ceramide (Table 1). The

second-order rate constant for the reaction of LUnAR RhoVR 1 with TCO-PEG$_{25}$-Halo is 150 (±10) M^{-1} s^{-1}, which similar to previously reported values for tetrazines bearing a methyl substituent, which range from 40[20] to 800 M^{-1} s^{-1}.[31]

We first tested a HaloTag targeting system for targeting LUnAR RhoVRs to both the exterior and interior leaflets of the plasma membrane. TCO tethered to a HaloTag chloroalkane ligand via a flexible polyethyleneglycol (PEG) linker would first be localized to HaloTag. Then, treatment with LUnAR RhoVR would result in labeling of HaloTag proteins (Scheme 1). LUnAR RhoVR1 labels the plasma membrane when HaloTag is localized to the outer leaflet of the plasma membrane (Figure S3a–c); however, when HaloTag is localized to the endomembrane via prenylation[35] (Figure S4), we observe very low levels of cellular fluorescence, likely because the long PEG linkers used to ensure voltage sensitivity of RhoVRs in HaloTag targeted systems[34] prevent substantial internalization of RhoVR (Figure S3d–f). Labeling of cells expressing the same endomembrane HaloTag show robust fluorescence when labeled with the cell-permeable JF646-HaloTag ligand, supporting this hypothesis (Figure S3f–h).

We verified the voltage-sensitivity of the product of LUnAR RhoVR 1 and TCO by reacting TCO-PEG$_{25}$-Halo (**25**) with LUnAR RhoVR 1 *in vitro* and applying this to cells expressing outer leaflet HaloTag (Figure S5).[34] Patch clamp electrophysiology on these cells reveal that LUnAR RhoVR 1 / TCO conjugates respond to membrane potential change, with a sensitivity of approximately 21% (± 0.72%, S.E.M. for n = 3 cells, Figure S5).

After establishing the voltage sensitivity of LUnAR RhoVR1-TCO conjugates at the outer leaflet of the plasma membrane, we turned to the organelle specific lipid-TCO developed by the Schepartz lab for their High Density Environmentally-sensitive probes (HIDE probes)[36] to target LUnAR RhoVRs to organelles. We loaded HeLa cells with a ceramide-TCO (Cer-TCO) followed by loading with LUnAR RhoVR 1 or LUnAR RhoVR 0 at 37 °C. We previously showed that, at temperatures below 20 °C Cer-TCO enables selective labeling of the Golgi with quenched tetrazine fluorophores.[37] However, when loaded at 37 °C, Cer-TCO enables labeling in the ER and Gogli.[36]

Cell treated with Cer-TCO followed by LUnAR RhoVR 1 show strong fluorescence associated with internal structures (Figure 2a, Figure S6, S8). Cells that pre-treated with Cer-TCO prior to LUnAR RhoVR treatment are significantly brigher than cells without Cer-TCO (up to 4.4× brighter, mean of 2.3× brighter; $p = 4.1\times10^{-23}$, Figure S7). The bright LUnAR signal colocalizes with the ER (Pearson's coefficient of 0.82 ± 0.03 with ER Tracker Green, Figure 2d) and shows negilible plasma membrane staining (Pearson's coefficient of 0.33 ± 0.07 with membrane-associated BeRST,[38] Figure 2d, Figure S6). Similar colocalization analysis reveals much lower colocalization with mitochondria (when using MitoTracker Deep Red as a marker for mitochondria,[13, 39] 0.75 ± 0.02). Mitochondria (measured by MitoTracker Deep Red) and ER (ER Tracker Green) show substantial colocalization themselves (0.68 ± 0.04)(Figure S6, S9). Colocalization values are even lower for Golgi (using GalNAcT2 – BFP as Golgi marker, 0.47 ± 0.05).[40] Together, these data show localization primarily to the ER. The voltage insensitive control compound, LUnAR RhoVR 0, shows similar cellular localization (Figure S6, S9).

Having established that LUnAR RhoVR 1 can label the ER via reacting with pre-localized Cer-TCO (Figure 2) and that the reaction product of LUnAR RhoVR 1 + TCO is voltage sensitive (Figure S5), we next sought to determine whether LUnAR RhoVR 1 is voltage sensitive in the ER membrane. Because of the difficulty associated with patch clamp electrophysiological calibration of ER membrane potential in living cells, we modified a previously reported literature method for inducing voltage changes in intracellular membranes.[9] In our method (Figure 3a, Figure S10), cells loaded with LUnAR RhoVR1 targeted to the ER via Cer-TCO are first treated briefly with digitonin to selectively permeabilize the cell membrane, but not organelle membranes. Digitonin permeabilizes cholesterol-rich membranes.[41] The plasma membrane contains up to 50% cholesterol content;[42–43] while ER membranes contain only about 5% cholesterol content.[44–45] Thus, the digitonin treatment selectively permeabilizes the plasma membrane while leaving the ER membrane intact.

We established plasma permeability by co-incubation with calcein-AM: cells with intact cell membranes retained calcein-AM fluorescence, while cells with permeabilized membranes showed little to no calcein fluorescence (Figure 3a).[46] After treatment with digitonin, cells are incubated in a buffer mimicking the intracellular environment (high $[K^+]$ of 130 mM) and containing the potassium ionophores valinomycin and nigericin which allows K^+ ions to equilibrate along their electrochemical gradient (Figure 3b).

Subsequently, a solution of low $[K^+]$ (10 mM) is perfused onto the cells (Figure 3c) while fluorescence images are taken over time (Figure 3e–h, S11). A short voltage transient is induced due to the different K^+ concentrations on either side of the ER membrane and high K^+ permeability induced by valinomycin and nigericin, resulting in a net negative potential on the luminal side of the ER (Figure 3c). Accompanying this hyperpolarization is a transient increase in LUnAR RhoVR 1 fluorescence of approximately 5% (Figure 3e). When a high $[K^+]$ solution is perfused back on the cells, the potential across the ER membrane is positive on the lumenal side (Figure 3d), and a small decrease in fluorescence occurs (Figure 3e). This response is likely smaller than the response to the initial hyperpolarization due to incomplete equilibration of the ER lumen with the low $[K^+]$ solution and thus a smaller magnitude of the reverse voltage transient.

The increase in fluorescence associated with ER lumen hyperpolarization is only observed in cells with permeabilized plasma membranes; non-permeabilized cells in the same dish, identified by their high intracellular calcein fluorescence, do not respond to differing $[K^+]$ perfusion (Figure 3f, Figure S12). In separate control experiments, perfusion with identical high $[K^+]$ solutions results in no fluorescence change (Figure 3g). Finally, if the high/low $[K^+]$ perfusion is repeated with voltage insensitive LUnAR RhoVR 0, we observe no change in fluorescence (Figure 3h). As an additional control confirm that LUnAR RhoVR 1 is not sensing mitochondrial membrane potential changes, we perfused FCCP, which transports protons across membranes down their concentration gradient,[47] rather than $[K^+]$. FCCP perfusion results in minimal fluorescence change (Figure S13). This supports localization of LUnAR RhoVR 1 to the ER, rather than mitochondria, and corroborates colocalization data (Figure 2, Figure S6, 7–8), since we previously established that low doses of FCCP (500 nM) cause a change in the mitochondrial membrane potential.[12] It further corroborates that

the fluorescence changes we observe upon switching [K^+] result from membrane potential changes in the ER, rather than off-target pH sensing, since the pH of the ER is similar to the cytosol,[1] while the pH gradient between the cytosol and other organelles like mitochondria and lysosome is much steeper.[1, 48] Finally, these data support localization of the majority of Cer-TCO/LUnAR RhoVR to the luminal leaflet of the ER membrane. An even distribution of Cer-TCO to cytosolic and luminal leaflets would give no response, but even a small bias for the luminal leaflet would give optical responses to ER membrane potential in the direction we observe. Taken together, these results demonstrate that LUnAR RhoVR 1 is able to sense voltage transients in the ER.

We next use LUnAR RhoVR1 to examine two physiological processes in which ER membrane potential changes may play a role: Ca^{2+} release from ER stores and electrical coupling between the ER and plasma membranes. We first examine ER voltage changes during Ca^{2+} release. The ER and sarcoplasmic reticulum (SR) are major cellular stores of calcium ions.[49] During cellular signaling processes, Ca^{2+} channels in the ER/SR open and Ca^{2+} is released from these internal stores,[49] moving down its electrochemical gradient and into the cytosol.[50]

The movement of Ca^{2+} out of the ER down its electrochemical gradient results in negative potentials in the ER lumen relative to the cytosol, unless cations enter the ER lumen to balance the charge. Potassium may flow into the ER lumen from the cytosol to compensate for the outward flow of Ca^{2+}. Previous reports find that SR membrane potential does not change during Ca^{2+} release.[51–52] However, the fluorescent reporters used in these experiments have limited time resolution due to their slower kinetics.[6–7, 53] VoltageFluors, because of their PeT mechanism, sense rapid changes in membrane potential,[33, 54] and thus we saw an opportunity to validate the conclusions of prior work by using LUnAR RhoVR to examine evidence for rapid changes in ER membrane potential in a non-excitable cell line.

Histamine treatment induces Ca^{2+} oscillations in HeLa cells which necessitates release of Ca^{2+} from internal stores.[55] By simultaneously measuring ER membrane potential in HeLa cells with LUnAR RhoVR 1/Cer-TCO at 200 Hz (Figure 4a) and Ca^{2+} oscillations via Oregon Green BAPTA (OGB, Figure 4b), we were able to look for rapid changes in ER voltage that could be linked to Ca^{2+} release. Intact cells were treated with Cer-TCO and LUnAR RhoVR 1 to label ER and OGB (Figure 4ab) and stimulated with histamine to evoke Ca^{2+} release. Fluorescence traces were then aligned so that the steepest increase in OGB fluorescence is synced to t = 0 in all traces (Figure S14). We observe no change from the baseline fluorescence of LUnAR RhoVR during histamine-evoked Ca^{2+} release when examining either individual cells (Figure 4c) or average responses across multiple trials (Figure 4d).

To establish a limit of detection, we developed an automated analysis routine (Figure S14). We examined each cell region of interest (ROI) to search for any cell on a coverslip that has a fluorescence change 10 standard deviations above the noise during the RhoVR recording. We then created artificial positives to test the limit of detection, increasing the fluorescence of an ROI at a single timepoint by 1 to 5% (Figure 4e). Then we asked what fraction of cells had detectable single-frame fluorescence changes. The unmodified data had no

cells with a detectable fluorescence change, but the automated analysis could readily detect changes of 2.5% or greater ($p < 0.001$, Student's t-test, 2-tailed unequal variance, Figure 4f). Taken together, these results extend the current literature hypothesis that voltage changes during Ca^{2+} release from the ER are not electrogenic and are likely compensated for by the movement of other ions into the ER. The more rapid time sensitivity of LUnAR RhoVR1 compared to existing probes rules out rapid voltage transients down to 5 ms in duration and <2.5% ΔF/F. The lower time bound is due to the limits of the image collection rate rather than the limits of probe response kinetics.

To further explore the ability of LUnAR RhoVR1 to measure biologically relevant voltage changes, we turned to patch-clamp electrophysiology to examine the electrical relationship between plasma membrane potential and ER membrane potential. A previous report using an internally targeted genetically-encoded voltage indicator (GEVI) gave evidence for electrical coupling and synchrony between the plasma membrane and internal membranes in HEK cells and hippocampal neurons.[10] Although optical signals from the plasma membrane and internal membranes moved in the opposite direction, the orientation of the GEVI in intracellular membranes is unknown; therefore, the direction of fluorescence change cannot be used to determine the direction of the voltage change. We set out to disambiguate the direction of the optical response and extend these results into another cell line through simultaneous electrical measurements of plasma membrane potential and optical measurements of ER membrane potential with LUnAR RhoVR 1. We induced plasma membrane depolarization (more positive inside) and hyperpolarization (more negative inside) in LUnAR RhoVR1 / Cer-TCO stained HeLa cells using whole-cell voltage clamp (Figure 5a).

Depolarizing steps in the plasma membrane (more positive potentials, Figure 5b) are accompanied by decreases in LUnAR RhoVR1 fluorescence (Figure 5c), which corresponds to a depolarization of the ER lumen (more positive on the inside). This result is consistent with $[K^+]$ perfusion experiments (Figure 3) and, along with the $[K^+]$ perfusion calibration, provides the first unambiguous confirmation of the correspondence of the sign of membrane potential change between ER and PM membrane potentials. Depolarization at the PM results in depolarization of the ER.

Notably, the fluorescence response of LUnAR RhoVR1 exactly follows the time course of the plasma membrane voltage command (Figure 5d, zoom-in of a single voltage step), suggesting a direct, or tight coupling of ER-PM potentials. When cells are stained with voltage insensitive LUnAR RhoVR0, the fluorescence does not change with membrane potential (Figure 5e/f), confirming that the observed fluorescence change with LUnAR RhoVR 1 is a response to ER membrane potential.

A two-color experiment with the plasma membrane potential reporter BeRST and LUnAR RhoVR 1 in Cer-TCO treated HeLa cells corroborates the electrophysiological recording. Depolarizing command voltages result in BeRST fluorescence increases (plasma membrane depolarization) and LUnAR RhoVR 1 fluorescence decreases (ER membrane depolarization) and are aligned precisely with the electrode-delivered plasma membrane potential command (Figure 5g).

Finally, a plot of the change in LUnAR RhoVR 1 fluorescence in the ER (ΔF/F) vs. the plasma membrane potential command reveals a plot with a substantial deviation from linearity. This is in contrast to the voltage sensitivity of pre-formed LUnAR RhoVR 1 on the plasma membrane of patch-clamped HEK cells, which shows a linear relationship between ΔF/F and plasma membrane command voltage (Figure S5e).

The ΔF/F response of LUnAR RhoVR 1 in the ER appears to have two linear components. At negative plasma membrane potentials (≤ 0 mV), we find a linear response of −1.4% per 100 mV (± 0.39, S.E.M., n = 5, R^2 = 0.997, Figure 5g). However, at positive potentials (> 0 mV), the ΔF/F voltage dependence becomes shallower: −0.4% per 100 mV (± 0.12, S.E.M., n = 5, R^2 = 0.97, Figure 5g). This greater than 3-fold change in the response at negative vs positive potentials is statistically significant (p = 0.037, paired t-test, n = 5, Figure S15). Because the fluorescence response of pre-formed LUnAR RhoVR on the plasma membrane is linear with respect to voltage (Figure S5e), this non-linear behavior may be due to underlying voltage changes in the ER. An intriguing possibility is that the ER rectifies, or opposes, plasma membrane potential commands at values more positive than 0 mV, and investigations are underway to explore the cellular and molecular mechanisms underlying this observation.

Conclusion

In this work, we report a new small-molecule sensor capable of targeting subcellular membranes. We show that LUnAR RhoVR is capable of targeting the ER of living cells and reporting on membrane potential fluctuations in this organelle in intact cells. This is the first report of a small molecule voltage dye used to measure ER potential dyanmics in intact cell; previous methods performed measurement in isolated membranes or vesicles.[5–7] Although the electrical properties measured in cell-free/isolated preparations of ER suggest that there is no potential difference across the ER,[56] recent reports show that synchrony exists between the plasma membrane potential changes and optical signals from an internal-membrane expressed GEVI.[10]

Using dual plasma membrane patch clamp and ER voltage imaging (Figure 5), we corroborate these previous observations and extend them into a new cell type. By combining patch clamp experiments with ionic calibration (Figure 3) and chemical targeting we directly establish that the directionality of the ER membrane potential change corresponds to the voltage change in the plasma membrane – meaning a depolarization at the plasma membrane (positive voltage outside) leads to a depolarization of the ER membrane (positive voltage in lumen). Further, our results reveal that ER membrane potential signals linearly track plasma membrane at negative potentials, but appear rectified at positive potentials. Further studies are geared towards exploring the nature of this functional coupling between the plasma membrane and ER membrane. We envision that LUnAR RhoVR will be an important addition to the suite of methods available for monitoring ER and other organelle physiology. Partnering LUnAR RhoVR with other lipid-based HIDE probes will allow access to the physiology of additional organelles.

Supplementary Material

Refer to Web version on PubMed Central for supplementary material.

ACKNOWLEDGMENT

E.W.M. acknowledges support from the Camille Dreyfus Teacher Scholar Awards program and the NIH (R35GM119855). P.E.Z.K., J.G.M., A.M.M.G., M.X.N., and L.L were supported in part by a training grant from the NIH (T32GM06698). L.L., N.D., and J.T. were supported by the NIH (R01GM131372 and R35GM134963 to A.S.) Confocal imaging experiments were conducted at the CRL Molecular Imaging Center, supported by the Gordon and Betty Moore Foundation. We thank Holly Aaron and Feather Ives for expert technical assistance. We thank Hasan Celik and the staff of the College of Chemistry NMR facility for expert technical assistance. Instruments in the CoC NMR Facility are supported in part by the NIH (S10OD024998).

REFERENCES

1. Grabe M; Oster G, Regulation of organelle acidity. J Gen Physiol 2001, 117 (4), 329–44. [PubMed: 11279253]
2. Kirichok Y; Krapivinsky G; Clapham DE, The mitochondrial calcium uniporter is a highly selective ion channel. Nature 2004, 427 (6972), 360–4. [PubMed: 14737170]
3. Mak DO; Vais H; Cheung KH; Foskett JK, Isolating nuclei from cultured cells for patch-clamp electrophysiology of intracellular Ca(2+) channels. Cold Spring Harb Protoc 2013, 2013 (9), 880–4. [PubMed: 24003193]
4. Zhong XZ; Dong XP, Lysosome electrophysiology. Methods Cell Biol 2015, 126, 197–215. [PubMed: 25665447]
5. Russell JT; Beeler T; Martonosi A, Optical probe responses on sarcoplasmic reticulum. Oxacarbocyanines. J Biol Chem 1979, 254 (6), 2040–6. [PubMed: 154518]
6. Beeler TJ; Farmen RH; Martonosi AN, The mechanism of voltage-sensitive dye responses on sarcoplasmic reticulum. J Membr Biol 1981, 62 (1–2), 113–37. [PubMed: 7277473]
7. Cabrini G; Verkman AS, Potential-sensitive response mechanism of diS-C3-(5) in biological membranes. J Membr Biol 1986, 92 (2), 171–82. [PubMed: 3761361]
8. Saminathan A; Devany J; Veetil AT; Suresh B; Pillai KS; Schwake M; Krishnan Y, A DNA-based voltmeter for organelles. Nat Nanotechnol 2021, 16 (1), 96–103. [PubMed: 33139937]
9. Matamala E; Castillo C; Vivar JP; Rojas PA; Brauchi SE, Imaging the electrical activity of organelles in living cells. Commun Biol 2021, 4 (1), 389. [PubMed: 33758369]
10. Sepehri Rad M; Cohen LB; Braubach O; Baker BJ, Monitoring voltage fluctuations of intracellular membranes. Sci Rep 2018, 8 (1), 6911. [PubMed: 29720664]
11. Deal PE; Kulkarni RU; Al-Abdullatif SH; Miller EW, Isomerically Pure Tetramethylrhodamine Voltage Reporters. J Am Chem Soc 2016, 138 (29), 9085–9088. [PubMed: 27428174]
12. Klier PEZ; Martin JG; Miller EW, Imaging Reversible Mitochondrial Membrane Potential Dynamics with a Masked Rhodamine Voltage Reporter. J Am Chem Soc 2021, 143 (11), 4095–4099. [PubMed: 33710896]
13. Johnson LV; Walsh ML; Chen LB, Localization of mitochondria in living cells with rhodamine 123. Proceedings of the National Academy of Sciences 1980, 77 (2), 990–994.
14. Zielonka J; Joseph J; Sikora A; Hardy M; Ouari O; Vasquez-Vivar J; Cheng G; Lopez M; Kalyanaraman B, Mitochondria-Targeted Triphenylphosphonium-Based Compounds: Syntheses, Mechanisms of Action, and Therapeutic and Diagnostic Applications. Chem Rev 2017, 117 (15), 10043–10120. [PubMed: 28654243]
15. Wang H; Fang B; Peng B; Wang L; Xue Y; Bai H; Lu S; Voelcker NH; Li L; Fu L; Huang W, Recent Advances in Chemical Biology of Mitochondria Targeting. Frontiers in Chemistry 2021, 9 (321).
16. Gao P; Pan W; Li N; Tang B, Fluorescent probes for organelle-targeted bioactive species imaging. Chem Sci 2019, 10 (24), 6035–6071. [PubMed: 31360411]

17. Tour O; Adams SR; Kerr RA; Meijer RM; Sejnowski TJ; Tsien RW; Tsien RY, Calcium Green FlAsH as a genetically targeted small-molecule calcium indicator. Nat Chem Biol 2007, 3 (7), 423–31. [PubMed: 17572670]
18. Bannwarth M; Corrêa IR; Sztretye M; Pouvreau S; Fellay C; Aebischer A; Royer L; Ríos E; Johnsson K, Indo-1 Derivatives for Local Calcium Sensing. ACS Chem Biol 2009, 4 (3), 179–190. [PubMed: 19193035]
19. Kamiya M; Johnsson K, Localizable and Highly Sensitive Calcium Indicator Based on a BODIPY Fluorophore. Analytical Chemistry 2010, 82 (15), 6472–6479. [PubMed: 20590099]
20. Gruskos JJ; Zhang G; Buccella D, Visualizing Compartmentalized Cellular Mg2+ on Demand with Small-Molecule Fluorescent Sensors. J Am Chem Soc 2016, 138 (44), 14639–14649. [PubMed: 27750004]
21. Best M; Porth I; Hauke S; Braun F; Herten D-P; Wombacher R, Protein-specific localization of a rhodamine-based calcium-sensor in living cells. Organic & Biomolecular Chemistry 2016, 14 (24), 5606–5611. [PubMed: 27072883]
22. Cañeque T; Müller S; Rodriguez R, Visualizing biologically active small molecules in cells using click chemistry. Nature Reviews Chemistry 2018, 2 (9), 202–215.
23. Knall AC; Slugovc C, Inverse electron demand Diels-Alder (iEDDA)-initiated conjugation: a (high) potential click chemistry scheme. Chem Soc Rev 2013, 42 (12), 5131–42. [PubMed: 23563107]
24. Chen W; Wang D; Dai C; Hamelberg D; Wang B, Clicking 1,2,4,5-tetrazine and cyclooctynes with tunable reaction rates. Chem Commun (Camb) 2012, 48 (12), 1736–8. [PubMed: 22159330]
25. Oliveira BL; Guo Z; Bernardes GJL, Inverse electron demand Diels–Alder reactions in chemical biology. Chem Soc Rev 2017, 46 (16), 4895–4950. [PubMed: 28660957]
26. Oliveira BL; Guo Z; Boutureira O; Guerreiro A; Jiménez-Osés G; Bernardes GJ, A Minimal, Unstrained S-Allyl Handle for Pre-Targeting Diels-Alder Bioorthogonal Labeling in Live Cells. Angew Chem Int Ed Engl 2016, 55 (47), 14683–14687. [PubMed: 27763724]
27. Wieczorek A; Werther P; Euchner J; Wombacher R, Green- to far-red-emitting fluorogenic tetrazine probes - synthetic access and no-wash protein imaging inside living cells. Chem Sci 2017, 8 (2), 1506–1510. [PubMed: 28572909]
28. Wu H; Yang J; Šečkutė J; Devaraj NK, In situ synthesis of alkenyl tetrazines for highly fluorogenic bioorthogonal live-cell imaging probes. Angew Chem Int Ed Engl 2014, 53 (23), 5805–9. [PubMed: 24764312]
29. Pinto-Pacheco B; Carbery WP; Khan S; Turner DB; Buccella D, Fluorescence Quenching Effects of Tetrazines and Their Diels–Alder Products: Mechanistic Insight Toward Fluorogenic Efficiency. Angewandte Chemie International Edition 2020, 59 (49), 22140–22149. [PubMed: 33245600]
30. Devaraj NK; Hilderbrand S; Upadhyay R; Mazitschek R; Weissleder R, Bioorthogonal turn-on probes for imaging small molecules inside living cells. Angew Chem Int Ed Engl 2010, 49 (16), 2869–72. [PubMed: 20306505]
31. Karver MR; Weissleder R; Hilderbrand SA, Synthesis and Evaluation of a Series of 1,2,4,5-Tetrazines for Bioorthogonal Conjugation. Bioconjugate Chemistry 2011, 22 (11), 2263–2270. [PubMed: 21950520]
32. Boggess SC; Gandhi SS; Siemons BA; Huebsch N; Healy KE; Miller EW, New Molecular Scaffolds for Fluorescent Voltage Indicators. ACS Chem Biol 2019, 14 (3), 390–396. [PubMed: 30735344]
33. Lazzari-Dean JR; Gest AM; Miller EW, Optical estimation of absolute membrane potential using fluorescence lifetime imaging. Elife 2019, 8, e44522. [PubMed: 31545164]
34. Deal PE; Liu P; Al-Abdullatif SH; Muller VR; Shamardani K; Adesnik H; Miller EW, Covalently Tethered Rhodamine Voltage Reporters for High Speed Functional Imaging in Brain Tissue. J Am Chem Soc 2020, 142 (1), 614–622. [PubMed: 31829585]
35. Choy E; Chiu VK; Silletti J; Feoktistov M; Morimoto T; Michaelson D; Ivanov IE; Philips MR, Endomembrane trafficking of ras: the CAAX motif targets proteins to the ER and Golgi. Cell 1999, 98 (1), 69–80. [PubMed: 10412982]
36. Takakura H; Zhang Y; Erdmann RS; Thompson AD; Lin Y; McNellis B; Rivera-Molina F; Uno SN; Kamiya M; Urano Y; Rothman JE; Bewersdorf J; Schepartz A; Toomre D, Long time-lapse

nanoscopy with spontaneously blinking membrane probes. Nat Biotechnol 2017, 35 (8), 773–780. [PubMed: 28671662]

37. Erdmann RS; Takakura H; Thompson AD; Rivera-Molina F; Allgeyer ES; Bewersdorf J; Toomre D; Schepartz A, Super-resolution imaging of the Golgi in live cells with a bioorthogonal ceramide probe. Angew Chem Int Ed Engl 2014, 53 (38), 10242–6. [PubMed: 25081303]
38. Huang YL; Walker AS; Miller EW, A Photostable Silicon Rhodamine Platform for Optical Voltage Sensing. J Am Chem Soc 2015, 137 (33), 10767–76. [PubMed: 26237573]
39. Scaduto RC Jr.; Grotyohann LW, Measurement of mitochondrial membrane potential using fluorescent rhodamine derivatives. Biophys J 1999, 76 (1 Pt 1), 469–77. [PubMed: 9876159]
40. Casler JC; Zajac AL; Valbuena FM; Sparvoli D; Jeyifous O; Turkewitz AP; Horne-Badovinac S; Green WN; Glick BS, ESCargo: a regulatable fluorescent secretory cargo for diverse model organisms. Mol Biol Cell 2020, 31 (26), 2892–2903. [PubMed: 33112725]
41. Stewart MP; Langer R; Jensen KF, Intracellular Delivery by Membrane Disruption: Mechanisms, Strategies, and Concepts. Chem Rev 2018, 118 (16), 7409–7531. [PubMed: 30052023]
42. Das A; Brown MS; Anderson DD; Goldstein JL; Radhakrishnan A, Three pools of plasma membrane cholesterol and their relation to cholesterol homeostasis. Elife 2014, 3, e02882.
43. Casares D; Escribá PV; Rosselló CA, Membrane Lipid Composition: Effect on Membrane and Organelle Structure, Function and Compartmentalization and Therapeutic Avenues. Int J Mol Sci 2019, 20 (9), 2167.
44. Ridsdale A; Denis M; Gougeon PY; Ngsee JK; Presley JF; Zha X, Cholesterol is required for efficient endoplasmic reticulum-to-Golgi transport of secretory membrane proteins. Mol Biol Cell 2006, 17 (4), 1593–605. [PubMed: 16452637]
45. Rossi AM; Taylor CW, IP(3) receptors - lessons from analyses ex cellula. J Cell Sci 2018, 132 (4), jcs222463. [PubMed: 30552138]
46. Lichtenfels R; Biddison WE; Schulz H; Vogt AB; Martin R, CARE-LASS (calcein-release-assay), an improved fluorescence-based test system to measure cytotoxic T lymphocyte activity. J Immunol Methods 1994, 172 (2), 227–39. [PubMed: 7518485]
47. Kalbácová M; Vrbacký M; Drahota Z; Melková Z, Comparison of the effect of mitochondrial inhibitors on mitochondrial membrane potential in two different cell lines using flow cytometry and spectrofluorometry. Cytometry A 2003, 52 (2), 110–6. [PubMed: 12655654]
48. Abad MF; Di Benedetto G; Magalhães PJ; Filippin L; Pozzan T, Mitochondrial pH monitored by a new engineered green fluorescent protein mutant. J Biol Chem 2004, 279 (12), 11521–9. [PubMed: 14701849]
49. Carreras-Sureda A; Pihán P; Hetz C, Calcium signaling at the endoplasmic reticulum: fine-tuning stress responses. Cell Calcium 2018, 70, 24–31. [PubMed: 29054537]
50. Goldman DE, POTENTIAL, IMPEDANCE, AND RECTIFICATION IN MEMBRANES. J Gen Physiol 1943, 27 (1), 37–60. [PubMed: 19873371]
51. Sanchez C; Berthier C; Allard B; Perrot J; Bouvard C; Tsutsui H; Okamura Y; Jacquemond V, Tracking the sarcoplasmic reticulum membrane voltage in muscle with a FRET biosensor. J Gen Physiol 2018, 150 (8), 1163–1177. [PubMed: 29899059]
52. Koshita M; Hotta K, Relationship between membrane potential and calcium ion fluxes in the fragmented sarcoplasmic reticulum. Jpn J Physiol 1981, 31 (1), 109–20. [PubMed: 6974268]
53. Tsutsui H; Karasawa S; Okamura Y; Miyawaki A, Improving membrane voltage measurements using FRET with new fluorescent proteins. Nat Methods 2008, 5 (8), 683–5. [PubMed: 18622396]
54. Beier HT; Roth CC; Bixler JN; Sedelnikova AV; Ibey BL, Visualization of Dynamic Sub-microsecond Changes in Membrane Potential. Biophys J 2019, 116 (1), 120–126. [PubMed: 30579565]
55. Vay L; Hernández-Sanmiguel E; Santo-Domingo J; Lobatón CD; Moreno A; Montero M; Alvarez J, Modulation of Ca(2+) release and Ca(2+) oscillations in HeLa cells and fibroblasts by mitochondrial Ca(2+) uniporter stimulation. J Physiol 2007, 580 (Pt 1), 39–49. [PubMed: 17234694]
56. Lam AKM; Galione A, The endoplasmic reticulum and junctional membrane communication during calcium signaling. Biochimica et Biophysica Acta (BBA) - Molecular Cell Research 2013, 1833 (11), 2542–2559. [PubMed: 23770047]

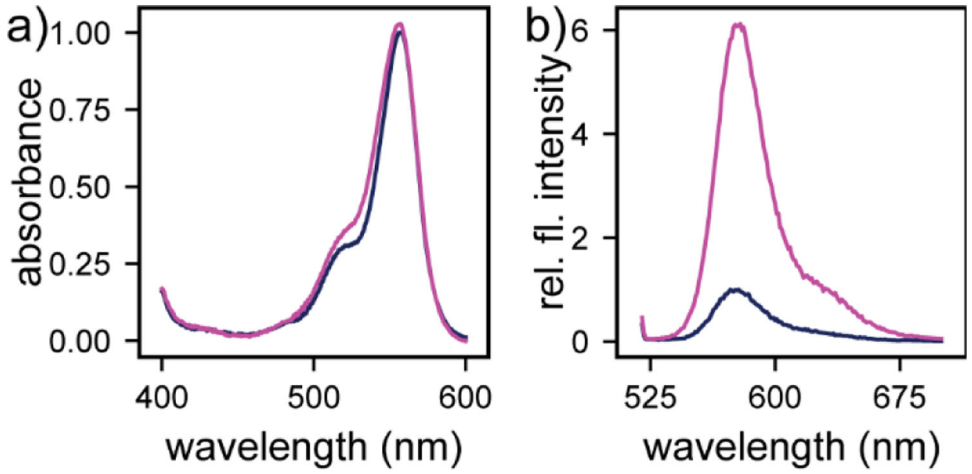

Figure 1.

Optical properties of LUnAR RhoVR before and after reaction with transcycloocteneol (TCO-ol). **a)** Plot of absorbance vs wavelength for LUnAR RhoVR1 before (dark blue) and after (magenta) reaction with transcycloocteneol. **b)** Plot of fluorescence emission vs. wavelength for LUnAR RhoVR 1 before (dark blue) and after (magenta) reaction with transcycloocteneol from the samples shown in **a**. Spectra were acquired in ethanol with 0.01% HCl. LUnAR RhoVR 1 (200 μM) was reacted with transcyclooctenol (10 mM) in 5:1 water:dioxane and then diluted to 500 nM for spectral measurements.

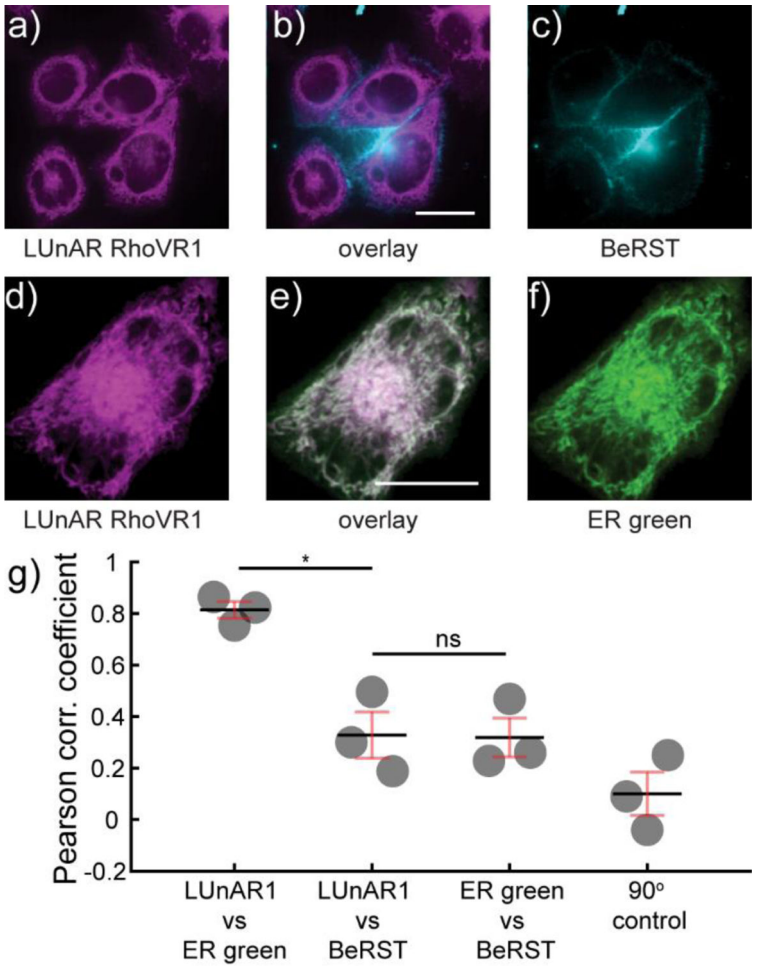

Figure 2.

LUnAR RhoVR 1 + Cer-TCO localize to the endoplasmic reticulum of HeLa cells. Confocal slices of HeLa cells pre-incubated with Cer-TCO followed by labeling with **a)** LUnAR RhoVR 1 (magenta) and **c)** the plasma membrane marker BeRST (cyan). **b)** An overlay of the two signals shows no significant overlap. Scale bar is 20 μm. Confocal slices of HeLa cells pre-incubated with Cer-TCO followed by labeling with **d)** LUnAR RhoVR 1 (magenta) and **f)** ER Tracker Green (green). **e)** An overlay of the two signals shows overlap in white. Scale bar is 20 μm. **d)** Plot of Pearson's coefficients for colocalization analysis of LUnAR RhoVR 1 and ER green or BeRST. 90° control indicates analysis in which one of the images has been rotated 90° during the colocalization analysis. * indicates $p < 0.05$; "ns" indicates $p > 0.05$ (student's t-test, two tailed unequal variance).

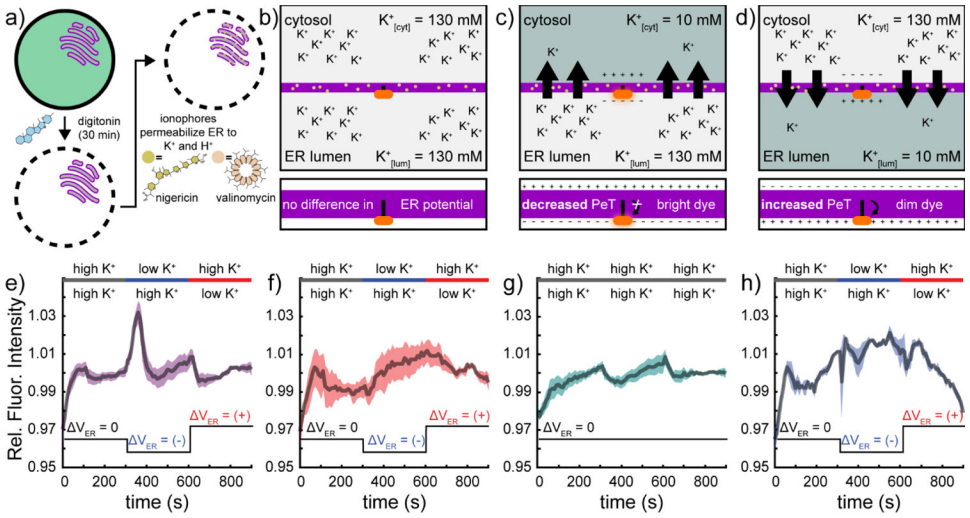

Figure 3.

LUnAR RhoVR1 senses voltage changes across the ER membrane. **a)** Schematic representation of permeabilization of plasma membranes with digitonin, resulting in loss of calcein fluorescence (green) but retention of LUnAR RhoVR1 staining in ER, treatment with ionophores valinomycin (beige) and nigericin (yellow), and modulation of $[K^+]$ to change ER membrane potential. **b)** When cytosolic and luminal $[K^+]$ is equal, there is no difference in membrane potential, and $\Delta V_{ER} \sim 0$. **c)** When the cytosolic $[K^+]$ is switched to 10 mM, valinomycin facilitates the diffusion of K^+ ions out of the ER lumen, resulting in a net negative luminal potential (ΔV_{ER} is negative), decreased PeT, and increased RhoVR fluorescence. **d**) When cytosolic $[K^+]$ is returned to 130 nM, K^+ again diffuses down its concentration gradient, resulting in a net positive luminal potential (ΔV_{ER} is positive), increased PeT, and decreased RhoVR fluorescence. **e-h**) Plots of relative RhoVR fluorescence intensity vs. time for Cer-TCO loaded, LUnAR RhoVR 1 stained HeLa cells with **e)** digitonin-permeabilized plasma membranes or **f)** intact plasma membranes. Grey bars indicate high $[K^+]$ (130 mM) in both cytosolic/external and luminal spaces, blue bars indicate low cytosolic/extracellular $[K^+]$ (10 mM) with high luminal $[K^+]$, and red bars indicate high cytosolic/external $[K^+]$ with low luminal $[K^+]$. **g)** Plot of relative RhoVR fluorescence intensity for cells as in (e), but with a constant high $[K^+]$ (130 mM) perfusion. **h)** Plot of relative RhoVR fluorescence intensity for cells as in (e), but with voltage-insensitive LUnAR RhoVR 0 in place of LUnAR RhoVR 1. Data represent mean values (solid lines) ± error (S.E.M.) for n = 9, 5, 4, or 3 for conditions e, f, g, and h, respectively. ΔV designations at the bottom of the plots indicate the relative potential across the ER membrane, relative to the lumen, where ΔV_{ER} = V (lumen) – V (cytosol).

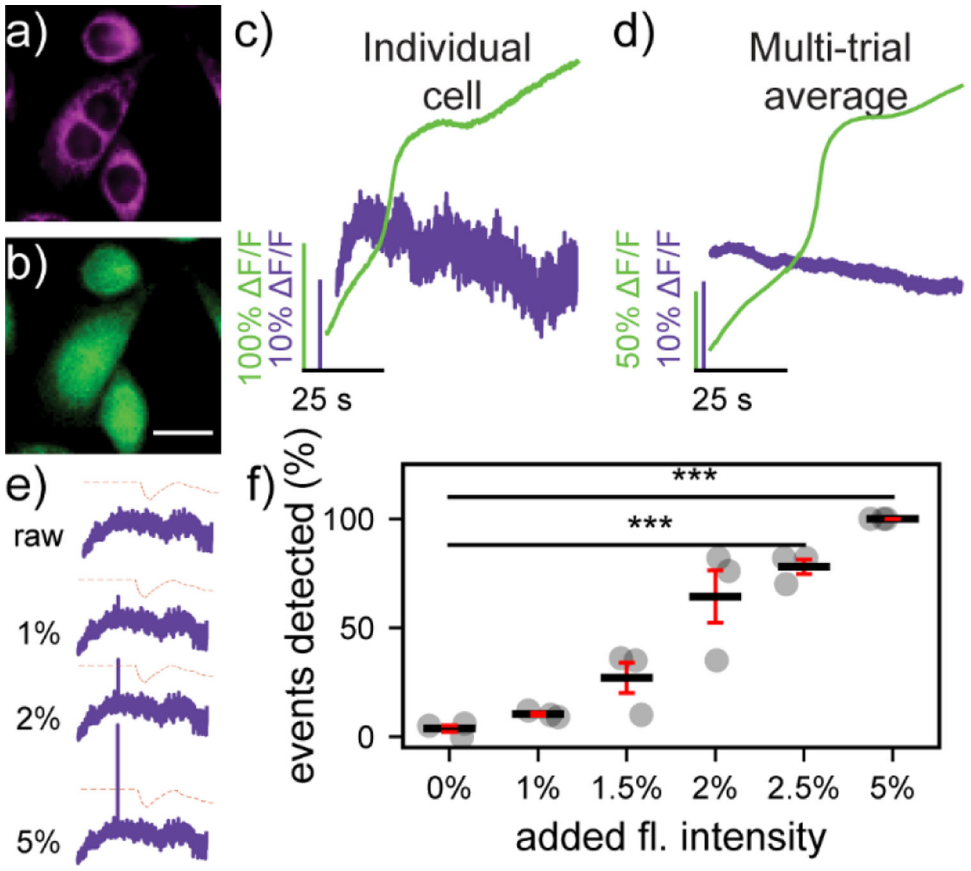

Figure 4.

ER membrane potential does not change during Ca^{2+} release in HeLa cells. **a)** Fluorescence image of HeLa cells treated with Cer-TCO and **a)** LUnAR RhoVR 1 to stain the ER and **b)** OGB-AM to visualize Ca^{2+} transients. Scale bar is 20 μm. Plots of LUnAR RhoVR 1 fluorescence (purple) and OGB fluorescence (green) vs time after histamine (100 μM) stimulation from a single HeLa cell 100 μM histamine stimulation (100 μM). Data are for either **c)** a single cell or **d)** the average across 3 different coverslips. **e**) Adding a fluorescence change of 0%, 1%, 2%, and 5% into the raw trace of a single cell (purple trace) and the threshold for 10 standard deviations above the local average fluorescence (dashed orange trace) used for detection. **f**) Plot of the fraction of individual cells in a single coverslip that have an event detected above the threshold shown in **c** on the raw fluorescence data from histamine trials as well as raw data where a single frame has an added fluorescence change of the amount indicated on the x-axis. *** indicates $p<0.001$ (student's t-test, 2-tailed, unequal variance)

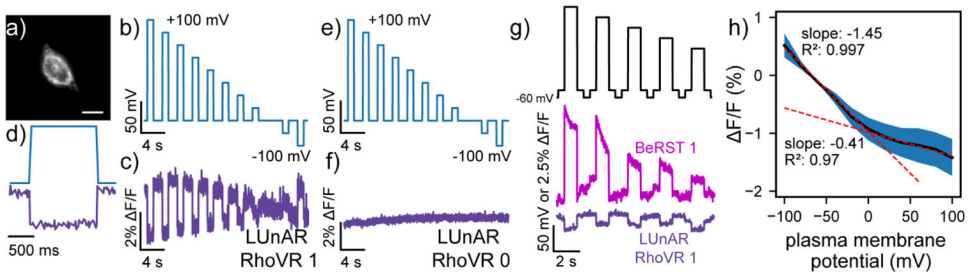

Figure 5.

Voltage imaging with LUnAR RhoVRs in the ER under whole-cell patch-clamp conditions. **a)** Widefield fluorescence image of HeLa cell treated with Cer-TCO, followed by LUnAR RhoVR 1. **b)** Plot of command voltage vs. time for patch-clamped HeLa cells with LUnAR RhoVR 1 labeling. **c)** Plot of LUnAR RhoVR 1 fluorescence vs. time for patch-clamped HeLa cells. **d)** Zoomed-in overlay of voltage command (blue) and LUnAR RhoVR 1 response (magenta) from panels b/c. **e)** Plot of command voltage vs. time for patch-clamped HeLa cells with LUnAR RhoVR 0 labeling. **f)** Plot of LUnAR RhoVR 0 fluorescence vs. time for patch-clamped HeLa cells. **g)** Two-color imaging of plasma membrane potential with BeRST 1 and ER membrane potential with LUnAR RhoVR 1. Black traces (upper) are the voltage commands, bright purple is BeRST 1, and magenta is LUnAR RhoVR 1. **h)** Plot of percent change in fluorescence from fluorescence at −60 mV as a function of plasma membrane potential from n=5 cells voltage clamped as in **a**. Error bars represent ± S.E.M. Dashed red lines are the line of best fit for values from −100 mV to 0 mV and from +20 mV to +100 mV.

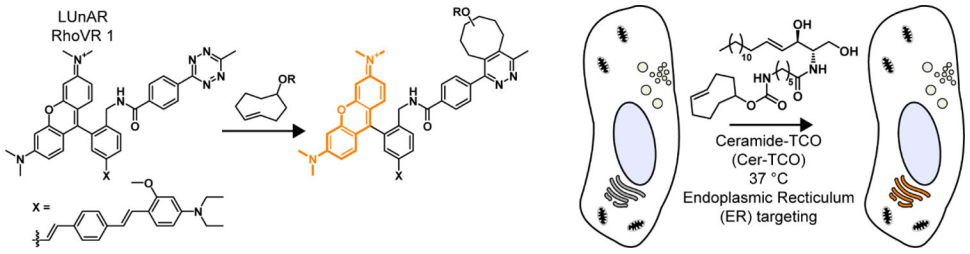

Scheme 1. Structures of LUnAR RhoVR and Cer-TCO for targeted delivery of RhoVRs to organelles

A small molecule rhodamine voltage sensor functionalized with a tetrazine quencher (LUnAR RhoVR 1) reacts with a targeted transcyclooctene (TCO) to form a covalent adduct with unquenched fluorescence. When this reaction is performed in live cells with a targeted transcyclooctene, for example ceramide-TCO, the small molecule voltage sensor is targeted to the membrane of interest with quenched fluorescence from any off-target localization.

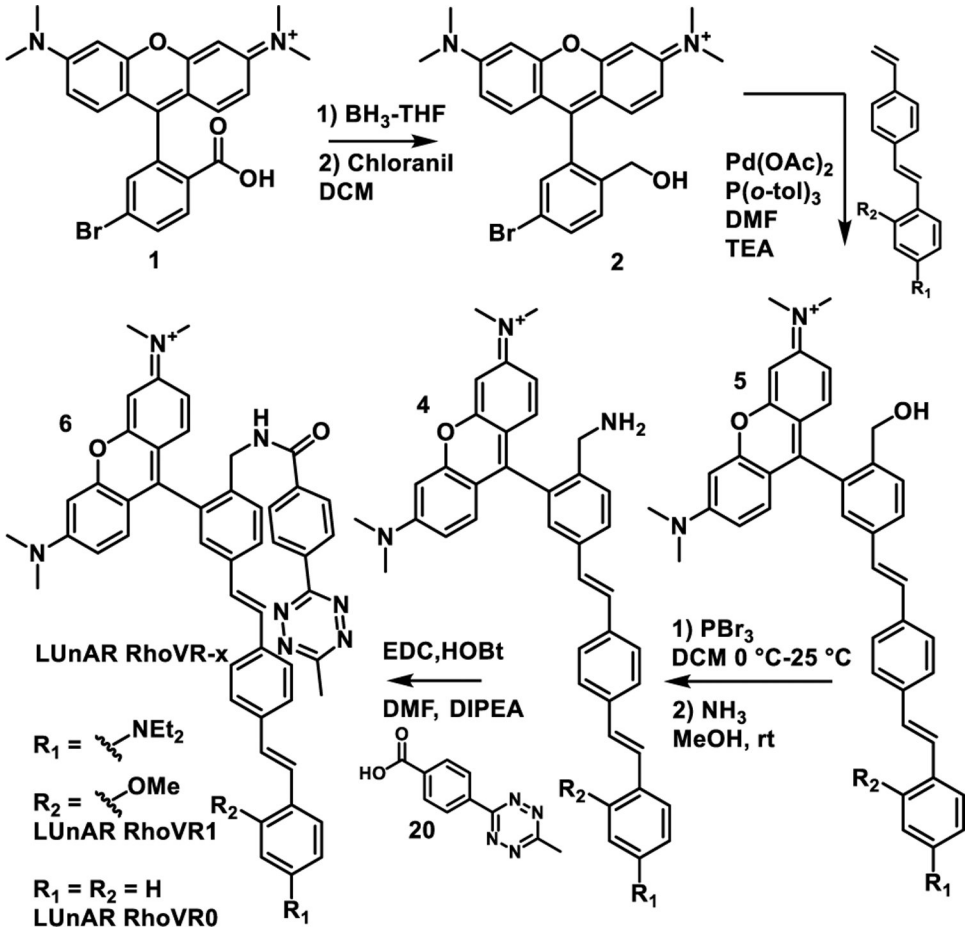

Scheme 2.
Synthesis of LUnAR RhoVRs

Table 1.

Reactions of LUnAR with Transcyclooctenes

RhoVR[a]	TCO	Φ_{fl}[b]
LUnAR **1**	---	0.042
LUnAR **1**	TCO-ol	0.26 (6.2×)
LUnAR **1**	TCO-PEG_{25}-Halo	0.28 (6.7×)
LUnAR **1**	Cer-TCO	0.20 (4.8×)
LUnAR **0**	---	0.032
LUnAR **0**	TCO-ol	0.32 (10.0×)
LUnAR **0**	Cer-TCO	0.17 (5.3×)

[a]The indicated LUnAR RhoVR (200 μM) was reacted with the indicated transcyclooctene (10 mM) in 5:1 water:dioxane and then diluted to 500 nM in ethanol with 0.01% HCl for spectral measurements.

[b]Quantum yield of fluorescence. Values in parenthesis indicate fold increase over unreacted RhoVR.